

## Electronic Supplementary Information

### Thienyltriazine based conjugated porous organic polymers: tuning of porosity and band gap, and CO<sub>2</sub> capture

Neha Rani Kumar<sup>a</sup>, Prasenjit Das<sup>b</sup>, Abhijeet R. Agrawal<sup>a</sup>, Sanjay K.Mandal<sup>b\*</sup>, and Sanjio S.  
Zade<sup>a\*</sup>

<sup>a</sup>*Department of Chemical Sciences, Indian Institute of Science Education and Research (IISER)  
Kolkata, Mohanpur 741246, India.*

<sup>b</sup>*Department of Chemical Sciences, Indian Institute of Science Education and Research Mohali,  
Sector 81, Manauli PO, S. A. S. Nagar, Mohali, Punjab 140306, India*

[\*] email: [sanjaymandal@iisermohali.ac.in](mailto:sanjaymandal@iisermohali.ac.in); [sanjiozade@iiserkol.ac.in](mailto:sanjiozade@iiserkol.ac.in)

## Table of Contents

Serial No.	Title	Page No.	
1	Experimental Section	a) General Instrumentation	S3
		b) Configurational Bias Monte Carlo (CBMC) molecular simulation	S4
		c) Materials	S4
		d) Synthesis of precursors used for polymerization; <b>Scheme S1</b>	S5
		e) Procedure for the synthesis of conjugated porous polymers( <b>TT-CPP1 to TT-CPP4</b> )	S6-S7
		f) Synthesis of <b>TT-CPP4</b> ; <b>Scheme S2</b>	S7
2	Characterization of synthesized porous polymers and monomers	a) Solid state <sup>13</sup> C NMR of <b>TT-CPP4</b> ; <b>Fig. S1</b>	S8
		b) IR spectrum of <b>TT-CPP4</b> ; <b>Fig.S2</b>	S8
		c) Stacked IR spectra of Precursor <b>1</b> and <b>TT-CPP1</b> ; <b>Fig. S3(a)</b>	S9
		d) Stacked IR spectra of Precursor <b>1, 2</b> and <b>TT-CPP2</b> ; <b>Fig. S3(b)</b>	S9
		e) Stacked IR spectra of Precursor <b>1</b> and <b>TT-CPP3</b> ; <b>Fig. S4(a)</b>	S10
		f) Stacked IR spectra of Precursor <b>3, 2</b> and <b>TT-CPP4</b> ; <b>Fig. S4(b)</b>	S10
		g) SEM Image of <b>TT-CPP4</b> ; <b>Fig. S5(a)</b> , TEM Image of <b>TT-CPP4</b> ; <b>Fig. S5(b)</b>	S10
		h) N <sub>2</sub> adsorption-desorption isotherm of <b>TT-CPP4</b> at 77K; <b>Fig. S6(a)</b> , Pore size distribution curve of <b>TT-CPP4</b> ; <b>Fig. S6(b)</b>	S11
		i) Powder diffraction pattern of <b>TT-CPP4</b> ; <b>Fig.S7</b>	S11
		j) TGA profile of <b>TT-CPP4</b> ; <b>Fig.S8</b>	S12
		k) Solid-state UV-Visible spectrum of <b>TT-CPP4</b> ; <b>Fig.S9</b>	S12
		l) Kubelka-Munk plot for band-gap calculation of <b>TT-CPP4</b> ; <b>Fig. S10</b>	S13
		m) Elemental analysis of <b>TT-CPP1 to TT-CPP4</b> ; <b>Table S1</b>	S13
		n) Stacked IR spectra of <b>TT-CPP (1-4)</b> after treatment with acid and base for 3 days; <b>Fig. S11</b>	S14
o) Recycling efficiencies of <b>TT-CPP1</b> for CO <sub>2</sub> uptake; <b>Fig. S12</b>	S14		
p) Summary of the CO <sub>2</sub> adsorption capacity data of various CPPs; <b>Table S2</b>	S15-S19		
3	NMR Spectra of precursors	a) <sup>1</sup> H NMR Spectrum of <b>C</b> ; <b>Fig.S13</b>	S20
		b) <sup>1</sup> H NMR Spectrum of <b>1</b> ; <b>Fig.S14</b>	S20
		c) <sup>1</sup> H NMR Spectrum of <b>3</b> ; <b>Fig.S15</b>	S21
14	References	S21	

## Experimental section

### General instrumentation

$^1\text{H}$  and  $^{13}\text{C}$  NMR spectra of the monomers and precursors were recorded at room temperature on a Jeol JNM-ECS 400 spectrometer (400 MHz  $^1\text{H}$ , 100 MHz  $^{13}\text{C}$ ) or Bruker Avance 500 (500 MHz  $^1\text{H}$ , 125 MHz  $^{13}\text{C}$ ) spectrometer with tetramethylsilane as the internal reference; chemical shifts ( $\delta$ ) are given in parts per million (ppm). Spectra were processed using MestReNova v5 and referenced to residual protonated solvent signals ( $\text{CDCl}_3$ :  $^1\text{H}$  7.26 ppm,  $^{13}\text{C}$  77.16 ppm). Fourier transform infrared spectroscopy (FTIR) spectra were recorded in the range of 4000-400  $\text{cm}^{-1}$  using the KBr pellet technique on a Perkin-Elmer RX1 IR Spectrometer. The thermal properties of CPPs were measured by thermogravimeter analyzer (Mettler Toledo, TGA/SDTA 851) from 40  $^\circ\text{C}$  to 800  $^\circ\text{C}$  at a heating rate of 10  $^\circ\text{C min}^{-1}$  under nitrogen atmosphere. A Rigaku (Mini Flex II, Japan) powder X-ray diffractometer having Cu  $K\alpha$  ( $\lambda = 1.54059 \text{ \AA}$ ) radiation was used to record the X-ray diffraction (XRD) patterns. Solid-state UV-vis absorption spectra were recorded on a JASCO V-670 spectrophotometer. Elemental analysis was performed using Perkin Elmer CHN analyzer. A Carl Zeiss SUPRA 55VP microscope was used to obtain the field-emission scanning electron microscopy (FESEM) images after coating the sample with Au film. Transmission electron microscopy (TEM) images were recorded with a JEOL JEM-2100F microscope at the Department of Science and Technology, Fund for Improvement of S&T Infrastructure in Higher Educational Institutions (DST-FIST) facility of IISER Kolkata. The  $^1\text{H}$ - $^{13}\text{C}$  CP/MAS NMR spectra were recorded on a Bruker AVANCE 500-MHz type ( $^1\text{H}$ , 500 MHz;  $^{13}\text{C}$ , 125 MHz) spectrometer at a spinning speed of 8 KHz and a relaxation delay of 10 seconds. UV-visible absorption spectra were recorded on an Agilent Cary60 UV-vis spectrophotometer.  $\text{N}_2$  adsorption-desorption isotherms were obtained on a Micromeritics Gemini VII surface area analyzer at 77 K and reported by Barrett-Joyner-Halenda surface/volume pore analysis. Samples were degassed at 120  $^\circ\text{C}$  under a  $\text{N}_2$  atmosphere for 12 h. The specific surface area was determined as per the Brunauer-Emmett-Teller (BET) method.  $\text{CO}_2$  sorption data were recorded for pressures in the range 0–1.2 bar by the volumetric method using a BELSORP MAX instrument. Isothermic heats of adsorption ( $Q_{st}$ ) were calculated using the Clausius-Clapeyron equation based on pure-component isotherms collected at three different temperatures of 273 K, 283 K and 298 K.  $Q_{st}$  is defined as:  $Q_{st} = -R(\partial \ln x / \partial (1/T))_y$ , where,  $x$  is the pressure,  $T$  is the

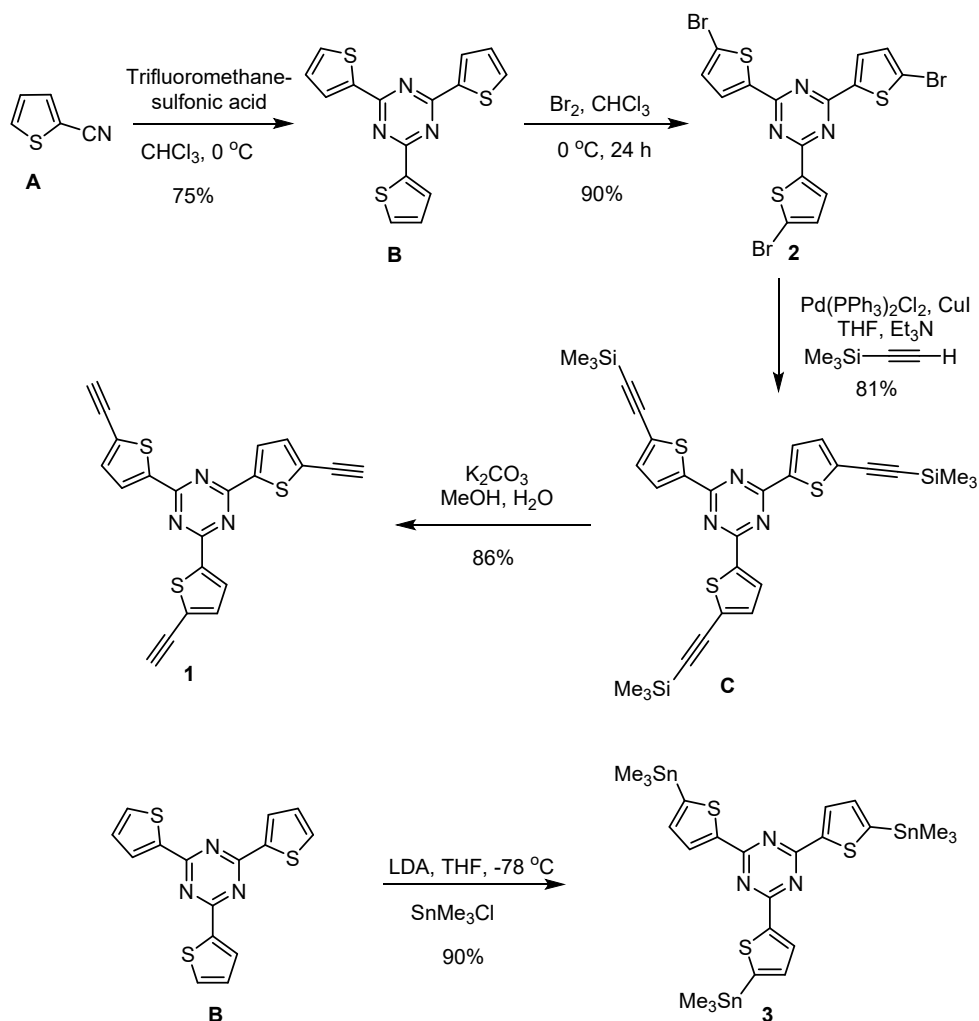
temperature,  $R$  is the gas constant and  $y$  is the adsorption amount. These calculations are done through the “Heat of Adsorption” function embedded in the Belsorp adsorption/desorption data analysis software version 6.3.1.0.

### **Configurational bias Monte Carlo (CBMC) molecular simulation<sup>1</sup>**

The structures of **TT-CPC-1,2,3** was assumed to be hexagonal rigid in the crystallographic position, which is obtained from single-crystal XRD data. The simulation boxes representing **TT-CPC-1,2,3** adsorbents consist of (1 x 1 x 1) unit cells for CO<sub>2</sub>. All the calculations were performed at different temperatures. Interatomic interactions were modelled with standard Lennard-Jones potential and Coulombic potentials. Lennard-Jones parameters between unlike atom types were computed using the Lorentz-Berthelot mixing rules. For the pairwise interactions between host-guest atoms of the particular force field, the nonbonding parameter has been utilized. The long-range part of electrostatic interactions was handled using the Ewald summation technique with a relative precision of 10<sup>-6</sup>. Periodic boundary conditions were applied in all three dimensions. For each state point, the CBMC simulation consists of 1 x 10<sup>7</sup> steps to guarantee equilibration, followed by 1 x 10<sup>7</sup> steps to sample the desired thermodynamic properties.

### **Materials**

All reagents were obtained from commercial sources (Sigma Aldrich, Spectrochem, Merck and Alfa Aesar) and used as received without further purification unless otherwise specified. Toluene and Tetrahydrofuran (THF) were dried over sodium/benzophenone before use. Dry reactions were conducted in oven-dried glassware using a standard Schlenk line under an inert atmosphere of dry nitrogen. Dimethylformamide (DMF) for polymerization reaction was dried over calcium hydride followed by distillation under vacuum. Triethylamine was dried over potassium hydroxide (KOH) flakes. Dichloromethane (DCM) and chloroform (CHCl<sub>3</sub>) were dried over calcium chloride. Solvents for Soxhlet extraction were used directly as obtained from commercial sources.



**Scheme S1.** Synthesis of the precursors used for polymerization.

2,4,6-tris(5-ethynylthiophen-2-yl)-1,3,5-triazine (**1**) was synthesized from 2-cyano thiophene (**A**) according to the procedure reported by Misra and the group.<sup>2</sup>  $^1\text{H}$  data of all the compounds were consistent with the reported values.  $^1\text{H}$  NMR of **1** (400 MHz, Jeol,  $\text{CDCl}_3$ ):  $\delta$  ppm 8.04 (d, 1H,  $J = 4$  Hz); 7.30 (d, 1H,  $J = 4$  Hz); 3.52 (s, 1H). Stannylation of compound **2** was carried out by using the method reported by Ogawa and the group.<sup>3</sup>  $^1\text{H}$  data of the compound matched with the reported data.  $^1\text{H}$  NMR of **3** (400 MHz, Jeol,  $\text{CDCl}_3$ ):  $\delta$  ppm 8.33 (d, 3H,  $J = 4$  Hz); 7.27 (d, 3H,  $J = 8$  Hz), 0.45 (s, 27H).

### **Procedure for the synthesis of TT-CPP1 [by the cyclotrimerisation reaction using $\text{Co}_2(\text{CO})_8$ catalyst]**

A 50 mL oven-dried three-neck round bottom flask fitted with a reflux condenser and a nitrogen purger on the top was charged with a small magnetic stirring bar. The reaction vessel was degassed and purged with nitrogen several times. The flask was then charged with 2,4,6-tris(5-ethynylthiophen-2-yl)-1,3,5-triazine (**1**) (1 g, 1 equiv) and 10 mL deoxygenated dioxane and the mixture was purged with nitrogen at room temperature for 20 minutes. In a separate single neck round-bottomed flask 10 mol % of dicobalt octacarbonyl,  $\text{Co}_2(\text{CO})_8$  was placed, followed by the addition of 5 mL of deoxygenated dioxane. The mixture was purged with nitrogen for 10 minutes. Meanwhile, the temperature of the flask containing the acetylene precursor **1** was set to 110 °C. After completion of purging, the solution of cobalt catalyst was added dropwise to the reaction mixture, and the refluxing was continued for 1.5 h. The reaction mixture was then cooled, and the crude reaction mixture was suspended in conc. HCl(aq) to remove metal residues and was purified with a successive Soxhlet extraction with water, methanol and ethanol. The polymer was further dried under vacuum for 3 h. Yield: 98%.

### **Procedure for the synthesis of TT-CPP2 (by the Sonogashira-Hagihara coupling reaction)**

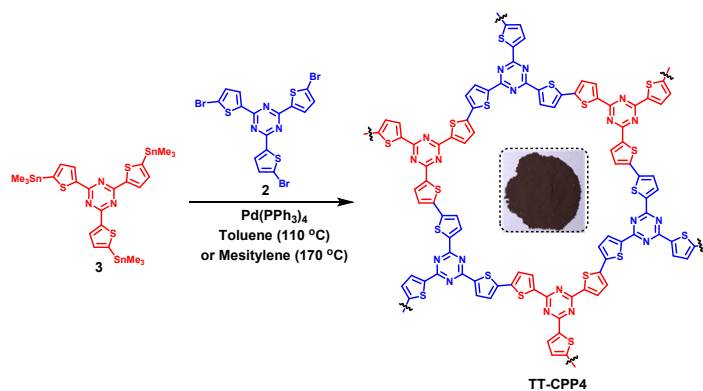
A 50 mL oven-dried three-neck round bottom flask fitted with a reflux condenser and a nitrogen purger on the top was charged with a small magnetic stirring bar. The reaction vessel was degassed and purged with nitrogen several times. Then the flask was charged with tribromo precursor (**2**, 0.67 equiv) and 2,4,6-tris(5-ethynylthiophen-2-yl)-1,3,5-triazine (**1**, 1 equiv). 7 mL anhydrous dimethylformamide (DMF) and 7 mL anhydrous triethylamine ( $\text{Et}_3\text{N}$ ) were added to the flask under nitrogen and then  $\text{Pd}(\text{PPh}_3)_4$  (5 mol%) and copper(I)iodide ( $\text{CuI}$ ), (5 mol%). The reaction mixture was stirred at 130 °C for 72 hours under a nitrogen atmosphere. The mixture was cooled to room temperature, and the precipitated polymer was filtered and washed three times with dichloromethane, water, methanol and acetone (100 mL each) to remove any unreacted monomers or catalyst residues. Further purification of the polymer was done by Soxhlet extraction with methanol and then  $\text{CHCl}_3$  for 24 hours each. The product was then dried under vacuum for 5 hours at 100 °C. Yield: 90%.

### Procedure for the synthesis of TT-CPP3 (by the Glaser coupling reaction)

A 50 mL oven-dried three-neck round bottom flask fitted with a reflux condenser under atmospheric condition was charged with a small magnetic stirring bar. The flask was then charged with 2,4,6-tris(5-ethynylthiophen-2-yl)-1,3,5-triazine (**1**) (0.45 g, 1 equiv) and 10 mL of Et<sub>3</sub>N and THF (1:1)mixture. This was followed by the addition of 5 mol% of Pd(PPh<sub>3</sub>)<sub>2</sub>Cl<sub>2</sub> and 5 mol% CuI. The mixture is then heated to 60 °C, and stirring continued as such for 72 hours. The mixture was cooled to room temperature, and the precipitated polymer was filtered and washed three times with dichloromethane, water, methanol and acetone (100 mL each) to remove any unreacted monomers or catalyst residues. Further purification of the polymer was done by Soxhlet extraction with methanol and then CHCl<sub>3</sub> for 24 hours each. The product was then dried under vacuum for 5 hours at 100 °C. Yield: 94%.

### Procedure for the synthesis of TT-CPP4 (by the Stille coupling reaction)

2,4,6-tris(5-(trimethylstannyl)thiophen-2-yl)-1,3,5-triazine (**3**) (0.5 g, 0.6 mmol, 1 equiv) and 2,4,6-tris(5-bromothiophen-2-yl)-1,3,5-triazine (**2**) (0.226 g, 0.4 mmol, 0.67 equiv), tetrakis(triphenylphosphine)palladium(0) (5 mol% with respect to **3**) and 5 mL of mesitylene were added to a two-neck flask fitted with a reflux condenser under an inert atmosphere. The solution was further purged with nitrogen for around 15 minutes, and then the solution was heated at 170 °C for 3 days with stirring. After the reaction, the solution was poured into methanol, and a red precipitate was collected by filtration. Then, the red powder was purified by Soxhlet extraction with methanol, dichloromethane, tetrahydrofuran, and acetone for 24 h each. Finally, the purified red powder was vacuum-dried for 3 h. Yield: 92%.



Scheme S2. Synthesis of TT-CPP4.

## Characterization of the synthesized polymers and monomers

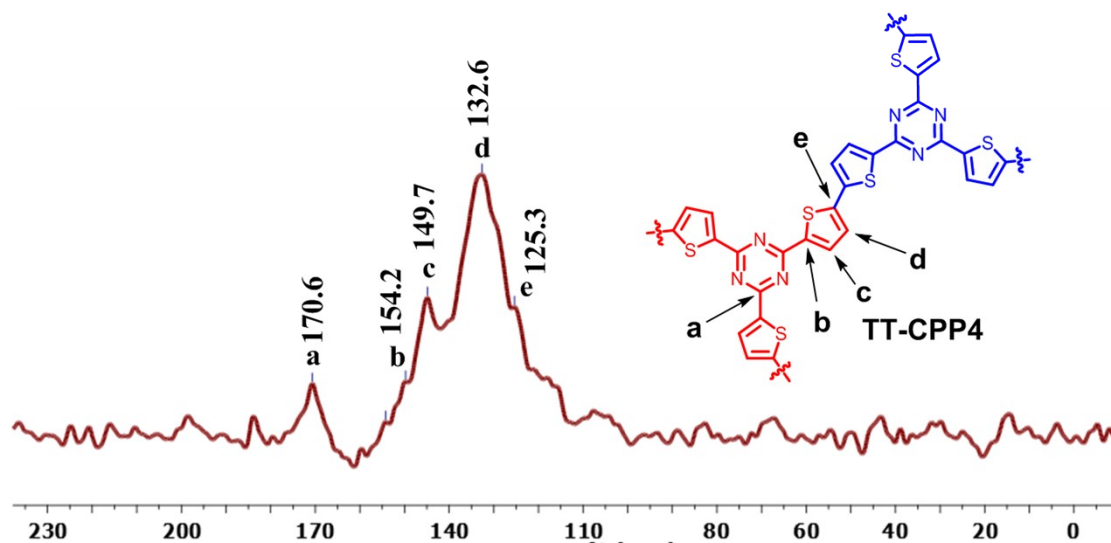


Fig. S1 Solid state CP-MAS $^{13}\text{C}$  NMR spectrum of TT-CPP4.

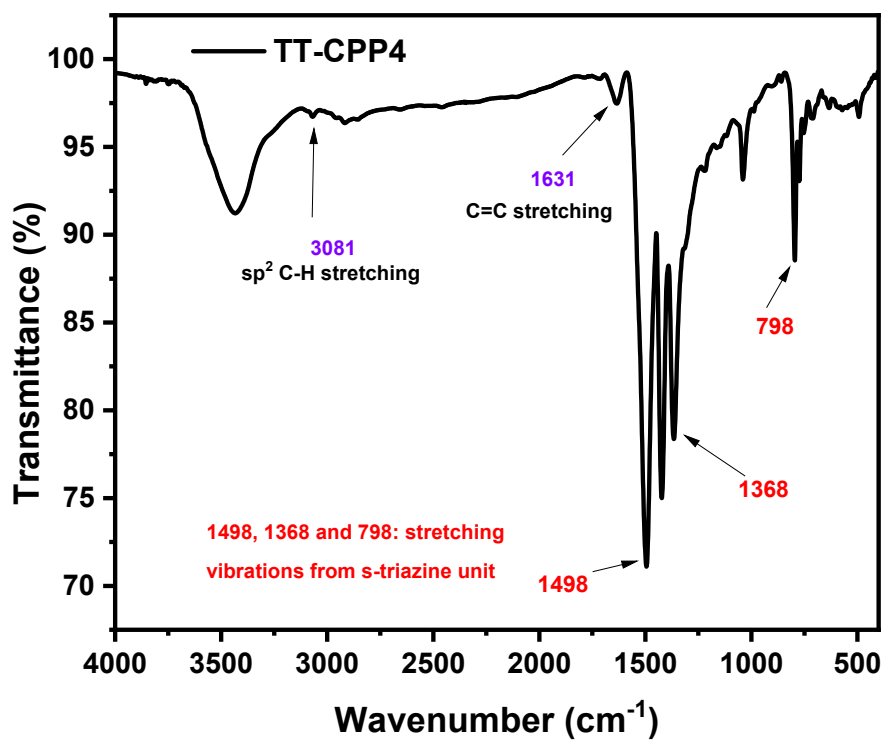
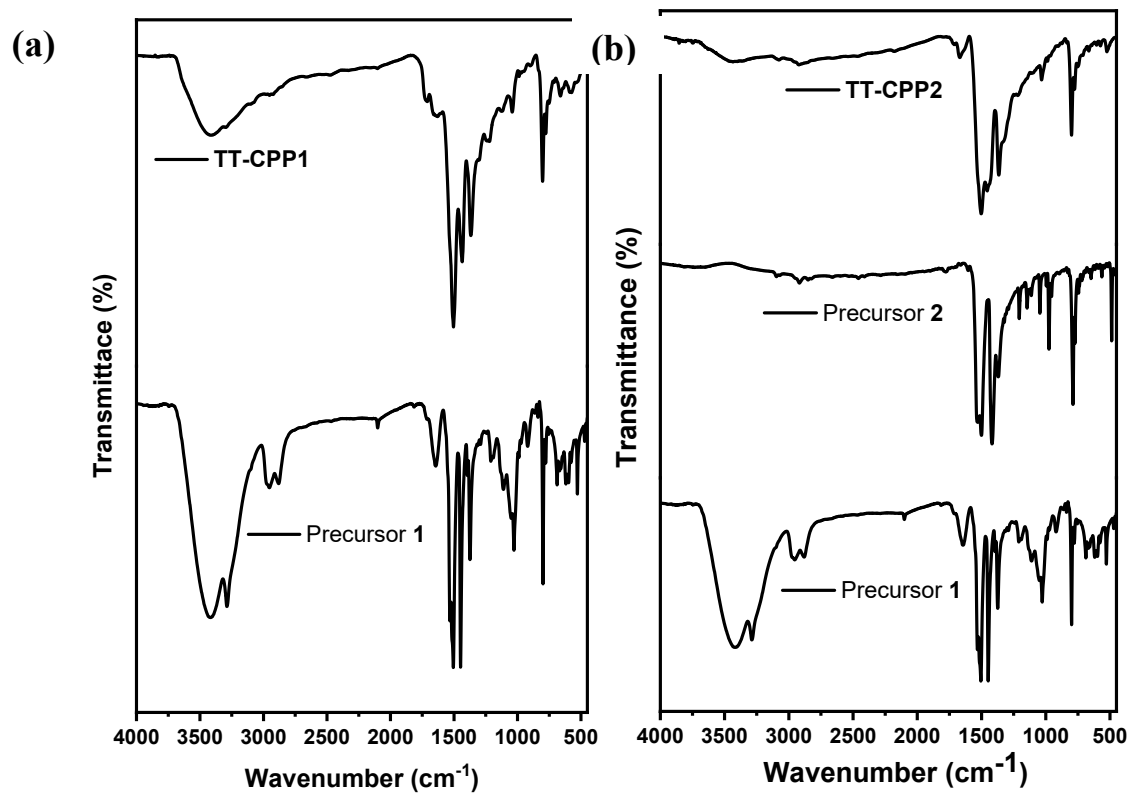
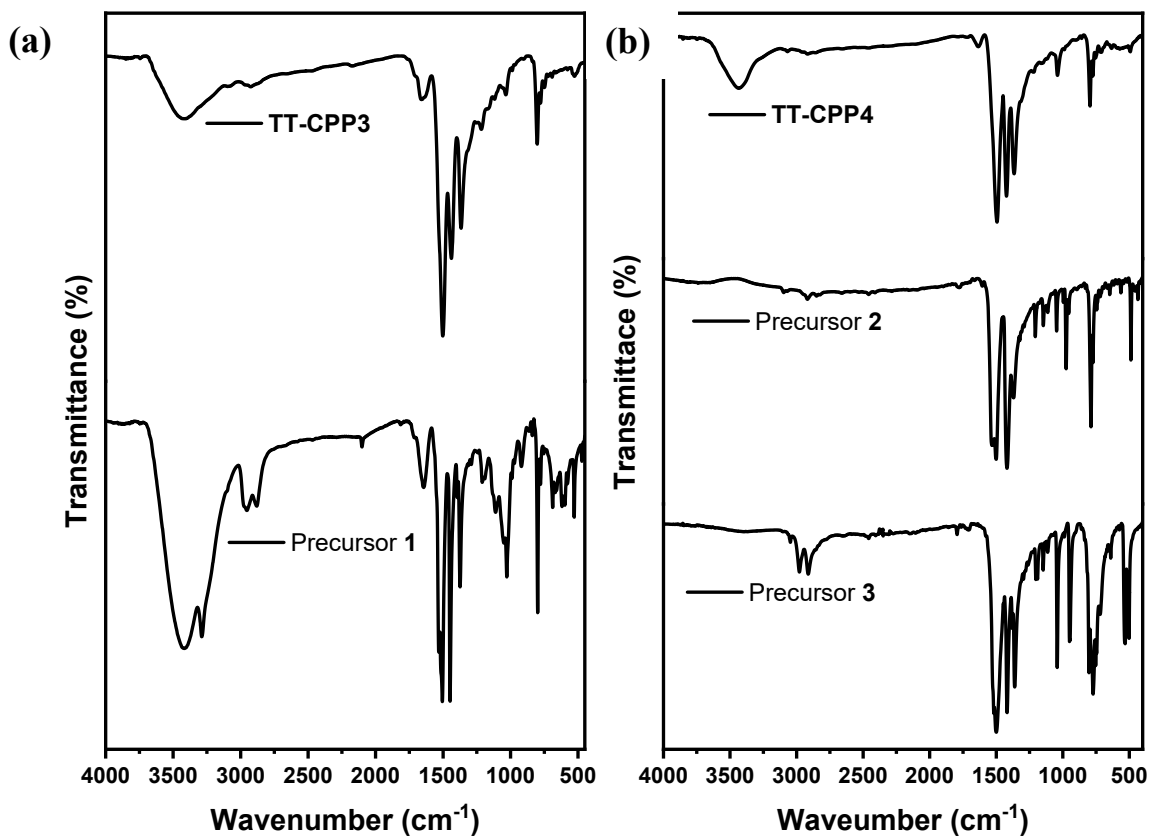


Fig. S2 FTIR spectrum of TT-CPP4.



**Fig. S3(a)** FTIR spectra of Precursor 1 and TT-CPP1 and **(b)** FTIR spectra of Precursor 1, 2 and TT-CPP2.



**Fig. S4** (a) FTIR spectra of Precursor 1 and TT-CPP3 and (b) FTIR spectra of Precursor 3, 2 and TT-CPP4.

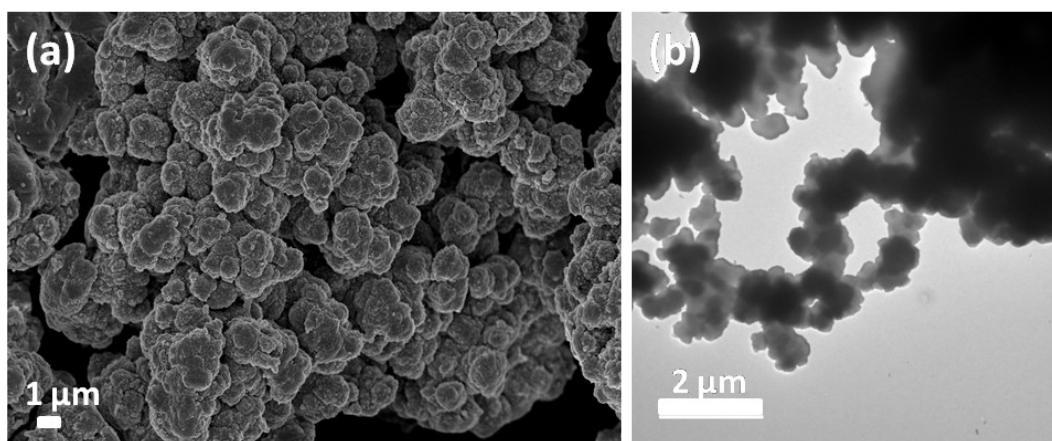


**Fig. S5** (a) SEM image of TT-CPP4 at  $1\ \mu\text{m}$  scale and (b) TEM image of TT-CPP4 at  $2\ \mu\text{m}$  scale.

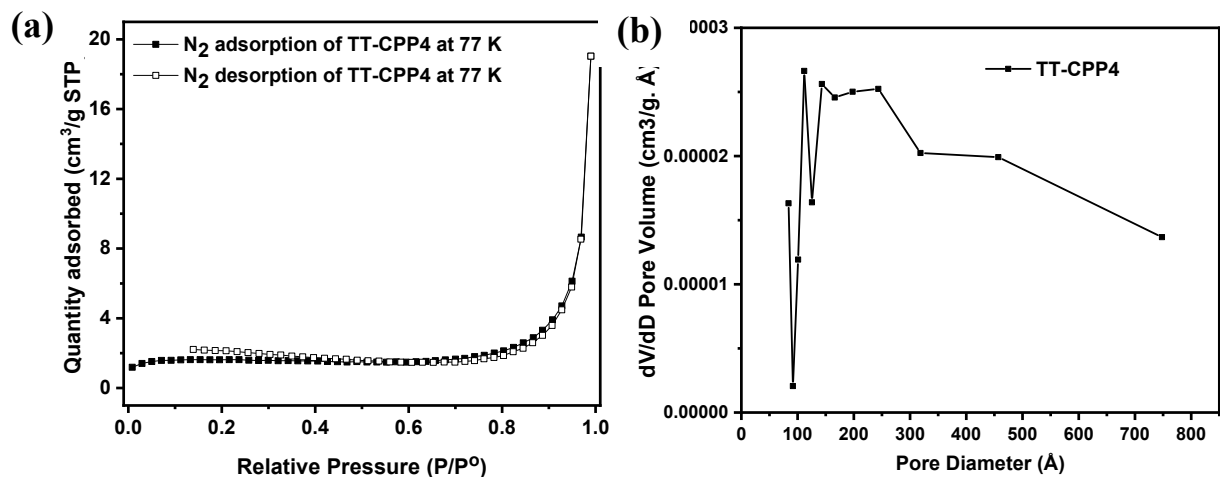


Fig. S6 (a) N<sub>2</sub> adsorption-desorption isotherm of TT-CPP4 at 77K and (b) Pore size distribution of TT-CPP4.

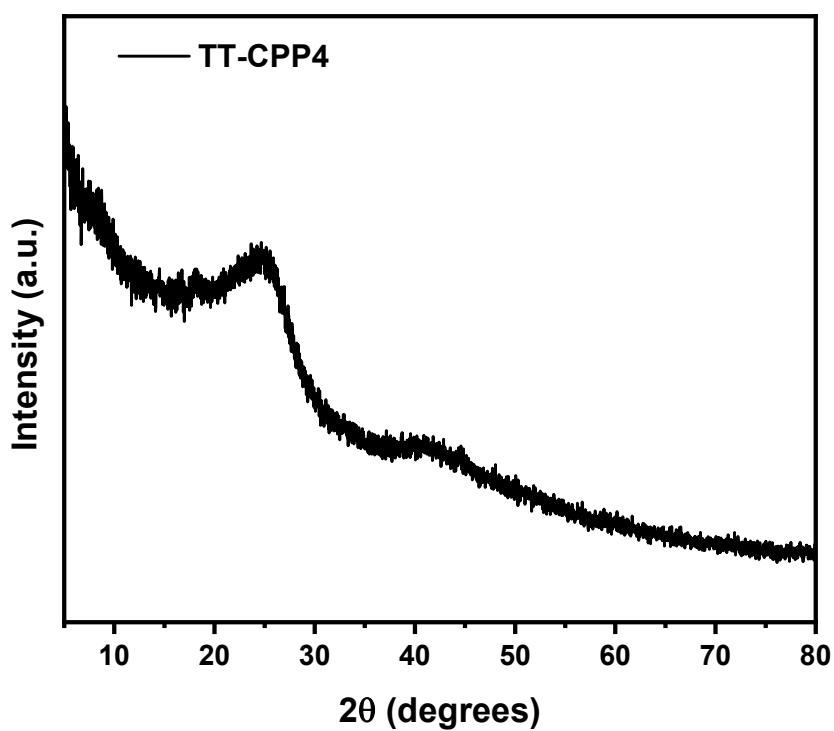


Fig. S7 Powder X-ray diffraction pattern of TT-CPP4.

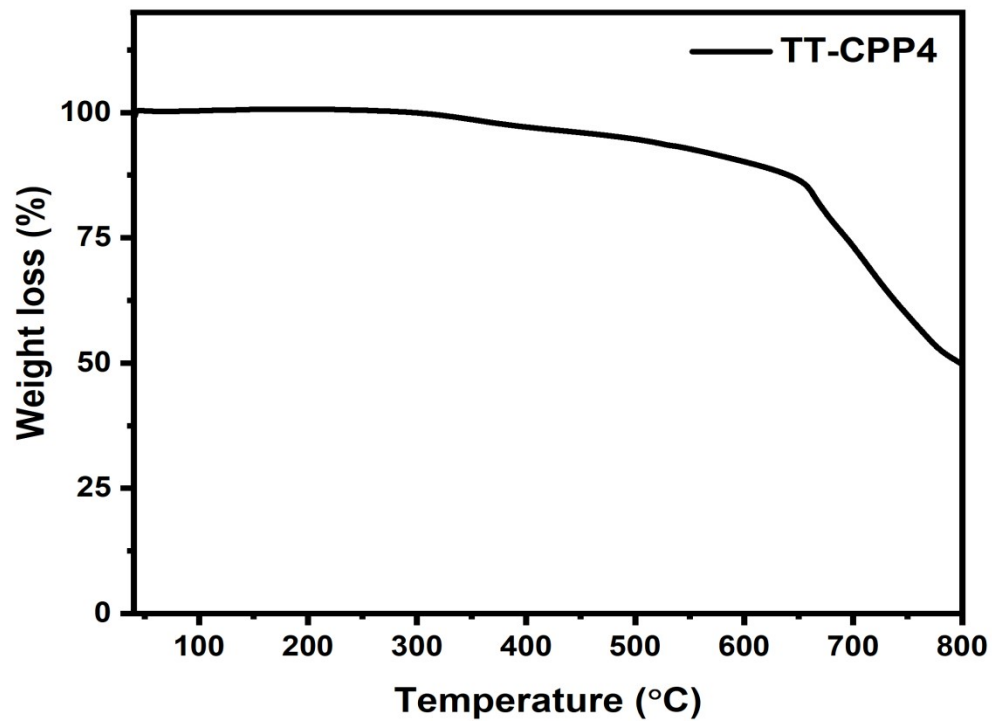


Fig. S8 TGA profile of TT-CPP4.

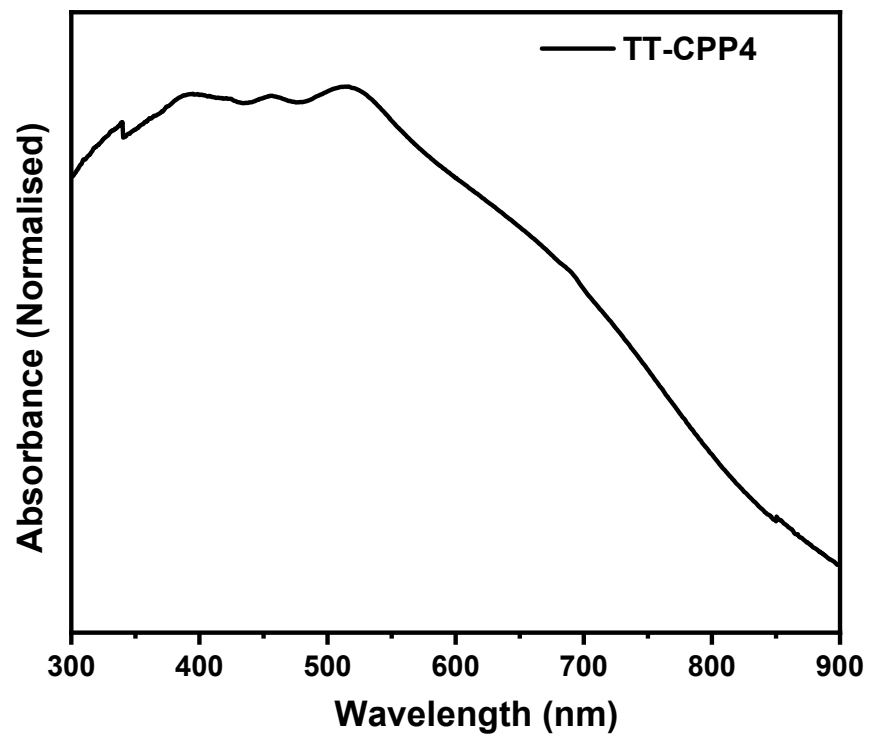


Fig. S9 Solid State UV-visible spectrum of TT-CPP4.

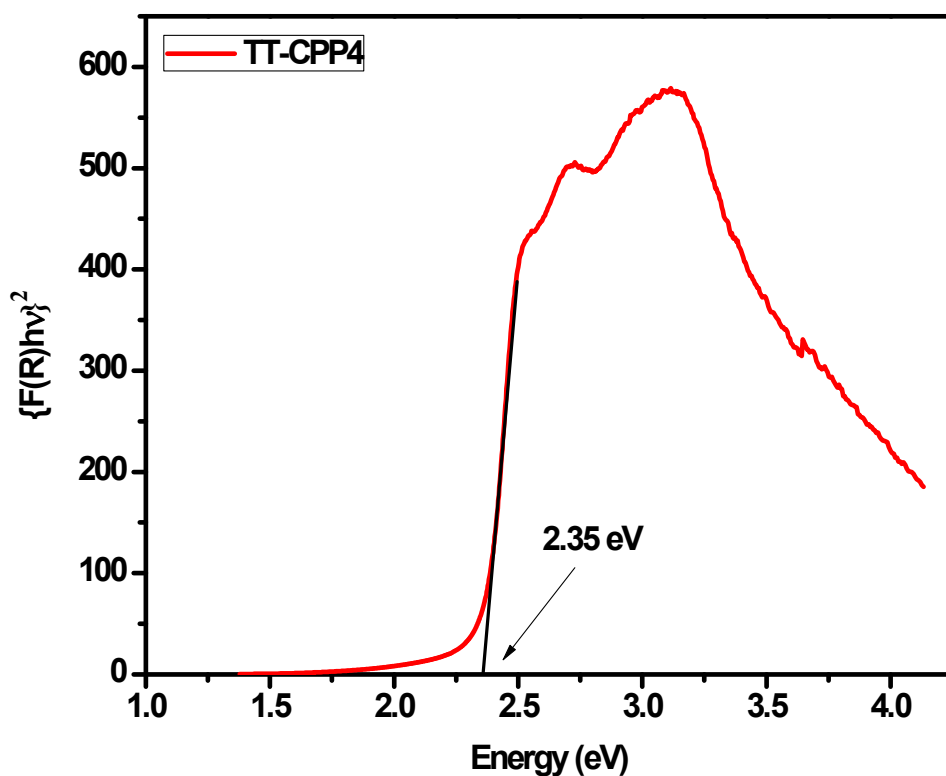
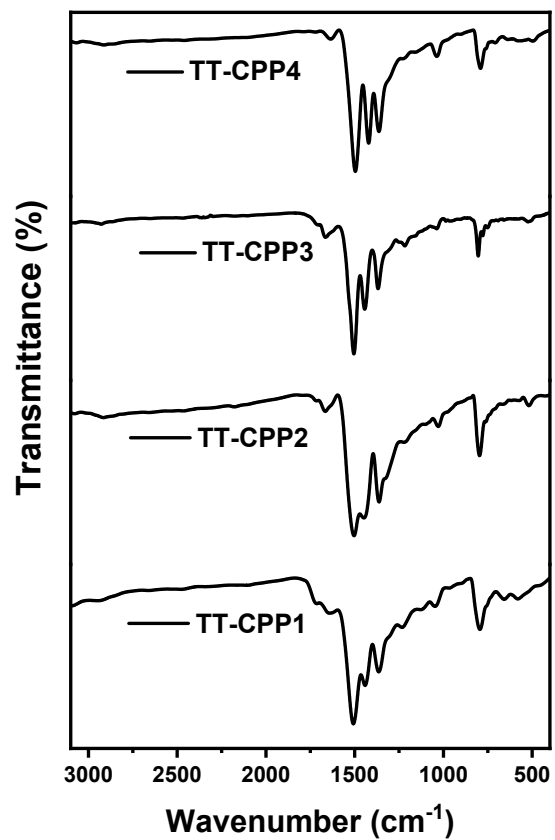


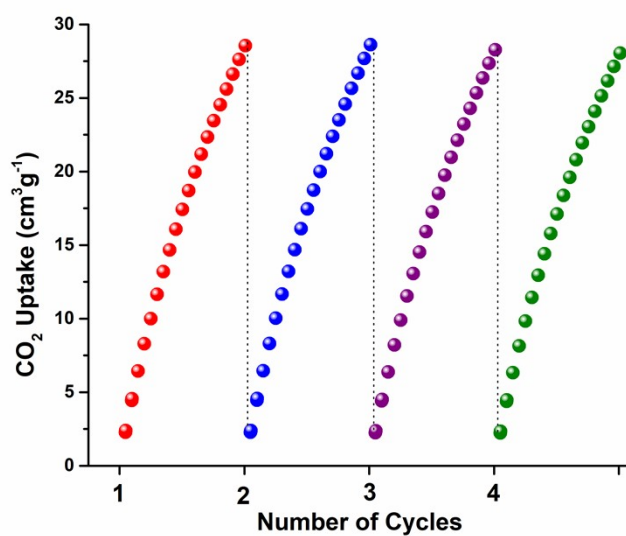
Fig. S10 Kubelka-Munk plot for band gap calculation of TT-CPP4.

Table S1. Elemental Analysis of TT-CPP1, TT-CPP2, TT-CPP3 and TT-CPP4.

Polymer	Theoretically calculated value	Experimental value
TT-CPP1 (C <sub>21</sub> H <sub>9</sub> N <sub>3</sub> S <sub>3</sub> )	C = 63.13, H = 2.27, N = 10.52	C = 58.91, H = 1.62, N = 8.41
TT-CPP2 (C <sub>40</sub> H <sub>12</sub> N <sub>6</sub> S <sub>6</sub> )	C = 62.48, H = 1.57, N = 10.93	C = 56.15, H = 1.21, N = 8.12
TT-CPP3 (C <sub>42</sub> H <sub>12</sub> N <sub>6</sub> S <sub>6</sub> )	C = 63.62, H = 1.53, N = 10.60	C = 60.08, H = 1.25, N = 8.01
TT-CPP4 (C <sub>30</sub> H <sub>12</sub> N <sub>6</sub> S <sub>6</sub> )	C = 55.53, H = 1.86, N = 12.95	C = 52.23, H = 1.31, N = 10.21



**Fig. S11** FTIR spectra of TT-CPP (1-4) after treatment with the organic solvent, acid, and base for 3 days.



**Fig. S12** Recycling efficiency of TT-CPP1 for CO<sub>2</sub> uptake.

**Table S2.** Summary of the CO<sub>2</sub> adsorption capacity data of various CPPs.

Entry	Material	S <sub>A</sub> BET (m <sup>2</sup> g <sup>-1</sup> )	Temperature (K)	Pressure (bar)	Adsorption capacity (mmol g <sup>-1</sup> )	Reference
1	TT-CPP1	545	263	1	2.62	<i>This work</i>
			273		2.18	
			298		1.27	
	TT-CPP2	511	263		1.75	
			273		1.63	
			298		1.08	
	TT-CPP3	491	263		1.42	
			273		1.22	
			298		0.76	
2	Py-azo-COP	700	273	1 15.5	1.93 4.14	<i>ACS Omega</i> , <b>2017</b> , <i>2</i> , 3572–3582.
3	Zn-CMP	791	298	1.01	1.33	<i>ChemSusChem</i> , <b>2014</b> , <i>7</i> , 2110–2114.
4	CMP1 CMP2	258	298	1	0.46	<i>Polymer</i> , <b>2016</b> , <i>90</i> , 187–192.
		567			0.67	
5	NWPTPE NWPPYR	508	298	1	0.68	<i>J. Polym. Sci., Part A: Polym. Chem.</i> , <b>2017</b> , <i>55</i> , 3862–3867.
		824			0.93	
6	HCTPP HCTPA HCTPM	582	273	1	2.79	<i>New J. Chem.</i> , <b>2017</b> , <i>41</i> , 3915–3919.
		921			2.27	
		670			2.14	
7	TCMP-0	963	273	1	2.38	<i>Polym. Chem.</i> , <b>2012</b> , <i>3</i> , 928–934.
			298		1.34	
	CMP-0	1018	273		2.1	
			298		1.21	
	TNCMP-2	995	273		2.62	
			298		1.45	
	TCMP-3	691	273		2.25	
			298		1.26	
	TCMP-5	494	273		1.22	
			298		0.68	
8	TPB-BD-CMP TPA-BD-CMP TPM-BD-CMP SPF-BD-CMP	657	273	1	2.5	<i>Mater. Chem. Front.</i> , <b>2017</b> , <i>1</i> , 867–872.
		543			2.94	
		1008			3.78	
		833			3.25	
9	P1 P2 P3	914	273	1	3.01	<i>Chem. Eur. J.</i> , <b>2016</b> , <i>22</i> , 7179–7183.
		834			2.53	
		873			2.12	
10	ACMP-C	629	195	1.06	11.14	<i>Macromolecules</i> , <b>2010</b> , <i>43</i> , 5508–5511.
			273		1.56	
			298		1.08	
	ACMP-C6	380	195		9.97	
			273		0.79	
			298		0.54	
	ACMP-N	46	195		11.5	
			273		1.16	
			298		0.79	
11	CMP1 CMP2 CMP3	767	273	1	2.94	<i>Macromolecules</i> , <b>2019</b> , <i>52</i> , 3935–3941.
		624			2.7	
		780			2.37	

12	<b>CMP-1-NH<sub>2</sub></b>	656	273 298	1	1.65 0.96	<i>Polymer</i> , <b>2014</b> , 55, 321–325.
	<b>CMP-1-AMD1</b>	316	273 298		1.51 0.96	
	<b>CMP-1-AMD2</b>	264	273 298		1.46 0.92	
	<b>CMP-1-AMD3</b>	119	273 298		1.31 0.83	
	<b>CMP-1-AMD4</b>	59	273 298		1.13 0.71	
	<b>CMP-1-AMD5</b>	37	273 298		1.1 0.64	
	<b>CMP-1-AMD9</b>	68	273 298		0.87 0.54	
13	<b>PP_CMP@mmm</b>	1928	273 298	1	2.52 1.36	<i>Chem. Commun.</i> , <b>2014</b> , 50, 2781–2783.
	<b>PP_CMP@omp</b>	43	273 298		0.82 0.43	
	<b>PP_CMP@omom</b>	81	273 298		1.05 0.66	
14	<b>Py-BF-CMP</b>	1306	273	1	3.21	<i>Macromolecules</i> , <b>2018</b> , 51, 3443–3449.
	<b>TPE-BF-CMP</b>	777	273		2.1	
	<b>TPA-BF-CMP</b>	590	273		1.83	
15	<b>HP<sub>E</sub>-CMP</b>	662	273 298	1	3.58 1.7	<i>RSC Adv.</i> , <b>2014</b> , 4, 6447–6453.
16	<b>CMP</b>	772	298	1.01	1.61	<i>Nat. Commun.</i> , <b>2013</b> , 4, 1960.
	<b>Co-CMP</b>	965			1.8	
	<b>Al-CMP</b>	798			1.74	
17	<b>Cr-CMP</b>	738	298	1.01	1.63	<i>J. Energy Chem.</i> , <b>2014</b> , 23, 22–28.
18	<b>Al-CMP</b>	839	273 298	1.01	0.98 0.62	<i>RSC Adv.</i> , <b>2015</b> , 5, 31664–31669.
19	<b>NCMP-I</b>	945	273 298	1	1.93 1.43	<i>Macromol. Mater. Eng.</i> , <b>2016</b> , 301, 451–456.
	<b>NCMP-III</b>	593	273 298		0.95 0.5	
20	<b>BQCMP-1</b>	422	273 298	1	1.55 1.06	<i>Macromol. Mater. Eng.</i> , <b>2016</b> , 301, 1104–1110.
	<b>DQCMP-1</b>	123	273 298		1.09 0.86	
21	<b>HCMP-1</b>	308	273	1	1.7	<i>Macromolecules</i> , <b>2016</b> , 49, 6322–6333.
	<b>HCMP-2</b>	58	273		1.23	
	<b>HCMP-3</b>	50	273		1.16	
	<b>HCMP-4</b>	28	273		0.98	
22	<b>PTEB aerogel</b>	1701	273	1	3.47	<i>Adv. Mater.</i> , <b>2014</b> , 26, 8053–8058.
23	<b>CMP-PM</b>	416	273	1.01	1.99	<i>Chem. Eur. J.</i> , <b>2018</b> , 24, 7480–7488.
	<b>CMP-PM-Me</b>	241	273		1.42	
24	<b>BO-CMP-1</b>	440	273	1	1.8	<i>Macromolecules</i> , <b>2018</b> , 51, 947–953.
	<b>BO-CMP-2</b>	1030			2.41	
	<b>oBO-CMP-1</b>	390			1.16	
	<b>oBO-CMP-2</b>	540			1.7	

25	<b>CMP-1</b> <b>CMP-1-(CH<sub>3</sub>)<sub>2</sub></b> <b>CMP-1-(OH)<sub>2</sub></b>	837 899 1043	298	1	1.18 0.94 1.07	<i>Chem. Sci.</i> , <b>2011</b> , 2, 1173–1177.
26	<b>BFCMP-1</b> <b>BFCMP-2</b>	1316 1470	273 298 273 298	1.13	2.45 1.39 2.77 1.64	<i>Polymer</i> , <b>2015</b> , 61, 36–41
27	<b>PPTBC</b> <b>PMTBC</b> <b>PPETBC</b> <b>PMETBC</b>	917 704 702 540	273 298 273 298 273 298 273 298	1.13	2.93 1.71 2.86 1.79 2.23 1.25 1.96 1.09	<i>Macromol. Chem. Phys.</i> , <b>2015</b> , 216, 504–510.
28	<b>MFCMP-1</b>	840	273	1	3.69	<i>J. Mater. Chem. A</i> , <b>2014</b> , 2, 13422–13430.
29	<b>CMP-YA</b> <b>CMP-SO-1B2</b> <b>CMP-SO-1B3</b>	1410 1085 1080	273 298 273 298 273 298	1	1.25 1.9 1.19 1.92 1.22 1.89	<i>Macromolecules</i> , <b>2017</b> , 50, 4993–5003.
30	<b>CK-COP-1</b> <b>CK-COP-2</b>	54 615	273	1	0.65 2.21	<i>J. Polym. Sci., Part A: Polym. Chem.</i> , <b>2017</b> , 55, 2383–2389.
31	<b>ThPOP-1</b> <b>ThPOP-2</b>	1050 160	273	1	3.41 0.91	<i>Polym. Chem.</i> , <b>2016</b> , 7, 5031–5038.
32	<b>Porp-TPE</b> <b>Porp-Py-CMP</b>	547 31	273 273	1.05 1.05	2.09 1.29	<i>Polym. Chem.</i> , <b>2019</b> , 10, 819–822.
33	<b>Por-Py-CMP</b>	1014	273 298	1	3 1.86	<i>RSC Adv.</i> , <b>2016</b> , 6, 75478–75481.
34	<b>DA-CMP1</b> <b>DA-CMP2</b> <b>Azo-CMP1</b> <b>Azo-CMP2</b>	662 603 1146 898	273 298 273 298 273 298 272 298	1.13	2.28 1.35 1.64 0.95 3.72 2.15 3.17 1.96	<i>J. Mater. Chem. A</i> , <b>2015</b> , 3, 21185–21193.
35	<b>SCMP-COOH@1</b> <b>SCMP-COOH@2</b> <b>SCMP-COOH@3</b>	911 622 820	298	1	1.39 1.07 1.25	<i>Polym. Chem.</i> , <b>2016</b> , 7, 4599–4602.
36	<b>ZnP-5N3-CMPs</b> <b>ZnP-25N3-CMPs</b> <b>ZnP-50N3-CMPs</b> <b>ZnP-75N3-CMPs</b> <b>ZnP-100N3-CMPs</b>	711 685 654 565 477	273 298 273 298 273 298 273 298	1	1 0.59 1.23 0.7 1.98 1.11 1.64 0.98 1.57 0.91	<i>Chem. Commun.</i> , <b>2017</b> , 53, 11422–11425.

	<b>ZnP-5F-CMPs</b>	430	273 298		1.32 0.77	
	<b>ZnP-25F-CMPs</b>	352	273 298		1.91 1.18	
	<b>ZnP-50F-CMPs</b>	240	273 298		2.95 2.04	
37	<b>PCZN-1</b> <b>PCZN-2</b> <b>PCZN-3</b> <b>PCZN-4</b> <b>PCZN-5</b> <b>PCZN-6</b> <b>PCZN-7</b> <b>PCZN-8</b> <b>PCZN-9</b> <b>PCZN-10</b>	1003 607 714 374 707 718 1058 1126 690 391	273	1	2.57 2.36 2.54 2.02 2.29 2.82 2.91 3.18 2.93 1.7	<i>Polym. Chem.</i> , <b>2017</b> , 8, 7240–7247.
38	<b>PCTF-8</b>	625	273 293	1	2.47 1.41	<i>J. Mater. Chem. A</i> , <b>2016</b> , 4, 13450–13457.
39	<b>BCMP3</b>	950	273 298	1	2.41 1.61	<i>Chem. Eur. J.</i> , <b>2015</b> , 21, 17355–17362.
40	<b>LKK-CMP-1</b>	467	273 298	1	2.22 1.38	<i>Ind. Eng. Chem. Res.</i> , <b>2018</b> , 57, 9254–9260.
41	<b>PCTF-1</b> <b>PCTF-2</b>	2235 784	273 298 273 298	1	3.22 1.84 1.82 0.99	<i>Chem. Commun.</i> , <b>2013</b> , 49, 3961–3963.
42	<b>CPOP-8</b> <b>CPOP-9</b> <b>CPOP-10</b>	1610 2440 1110	273	1	3.75 4.13 3.36	<i>Macromolecules</i> , <b>2014</b> , 47, 5926–5931.
43	<b>PTA-1</b> <b>PTA-2</b> <b>PTA-3</b>	52 62 450	273 273 303 273 303	1	0.84 1.25 0.59 1.48 0.77	<i>Chem. Commun.</i> , <b>2014</b> , 50, 8002–8005.
44	<b>BILP-101</b>	536	298	1	2.43	<i>Chem. Commun.</i> , <b>2015</b> , 51, 13393–13396.
45	<b>PAF-33</b> <b>PAF-33-NH<sub>2</sub></b> <b>PAF-33-COOH</b> <b>PAF-34</b> <b>PAF-34-OH</b> <b>PAF-35</b>	821 370 445 953 771 567	273 298 273 298 273 298 273 298 273 298	1	2.16 1.25 1.19 0.75 1.94 1.21 2.5 1.39 2.21 1.25 1.77 1.01	<i>Polym. Chem.</i> , <b>2014</b> , 5, 2266–2272.
46	<b>Cu/BF<sub>4</sub>/BIPLPL-1</b>	380	273	1	2.57	<i>J. Phys. Chem. C</i> , <b>2015</b> , 119, 8174–8182.
47	<b>BILP-15</b> <b>BILP-16</b> <b>BILP-15(AC)</b>	448 435 862	273 298 273 298 273	1	2.68 1.82 2.7 1.83 3.43	<i>Environ. Sci. Technol.</i> , <b>2015</b> , 49, 4715–4723.

	<b>BILP-16(AC)</b>	843	298 273 298		2.29 3.46 2.32	
48	<b>TBILP-1</b>	117	273 298	1	2.91 1.98	<i>Macromolecules</i> , <b>2014</b> , <i>47</i> , 8328–8334.
49	<b>BILP-10</b> <b>BILP-11</b> <b>BILP-13</b>	787 658 677	273 298 273 298 273 298	1	4.02 2.52 3.09 2 2.57 1.8	<i>J. Mater. Chem. A</i> , <b>2014</b> , <i>2</i> , 12492–12500.
50	<b>NPOF-1</b> <b>NPOF-1-NO<sub>2</sub></b> <b>NPOF-1-NO<sub>2</sub>(xs)</b> <b>NPOF-1-NH<sub>2</sub></b> <b>NPOF-1-NH<sub>2</sub>(xs)</b>	2062 1295 749 1535 1074	298	1	1.52 2.52 2 3.77 2.93	<i>J. Phys. Chem. C</i> , <b>2016</b> , <i>120</i> , 2592–2599.
51	<b>ALP-5</b> <b>ALP-6</b> <b>ALP-7</b> <b>ALP-8</b>	801 698 412 517	273 298 273 298 273 298	1	4.46 2.94 3.42 2.17 2.5 1.55 3.05 1.97	<i>J. Mater. Chem. A</i> , <b>2015</b> , <i>3</i> , 20586–20594.

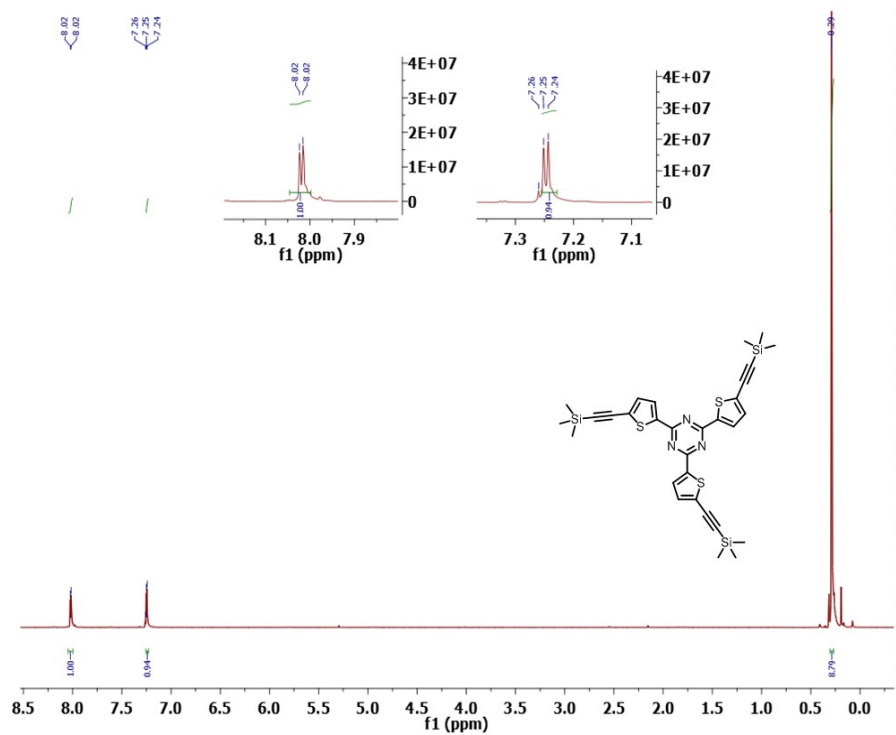


Fig. S13  $^1\text{H}$  NMR spectrum of C (400 MHz,  $\text{CDCl}_3$ ).

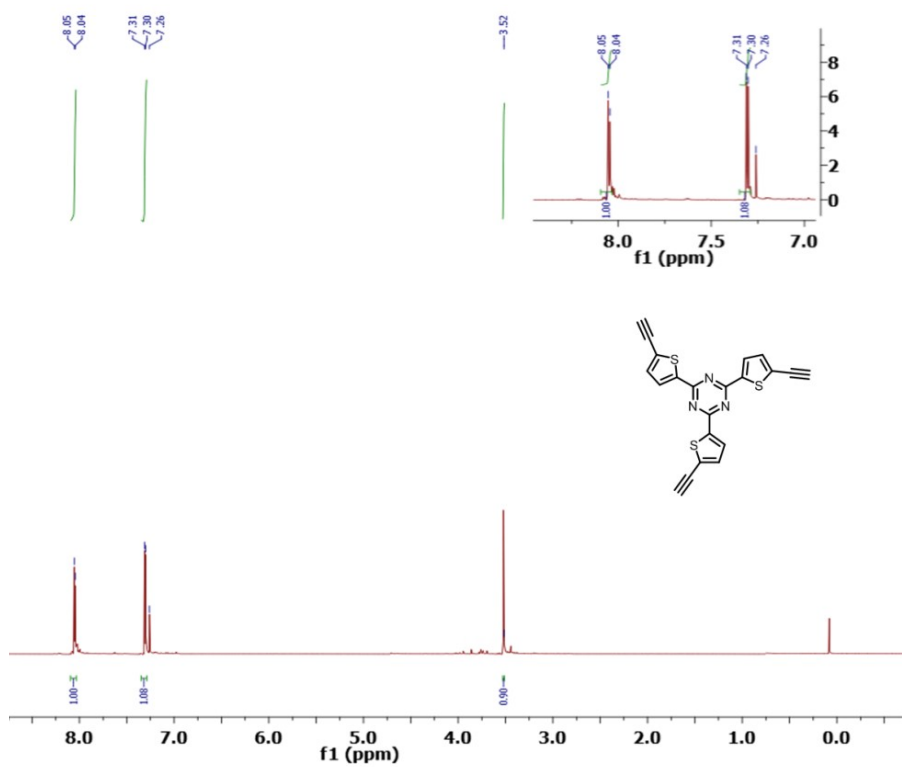
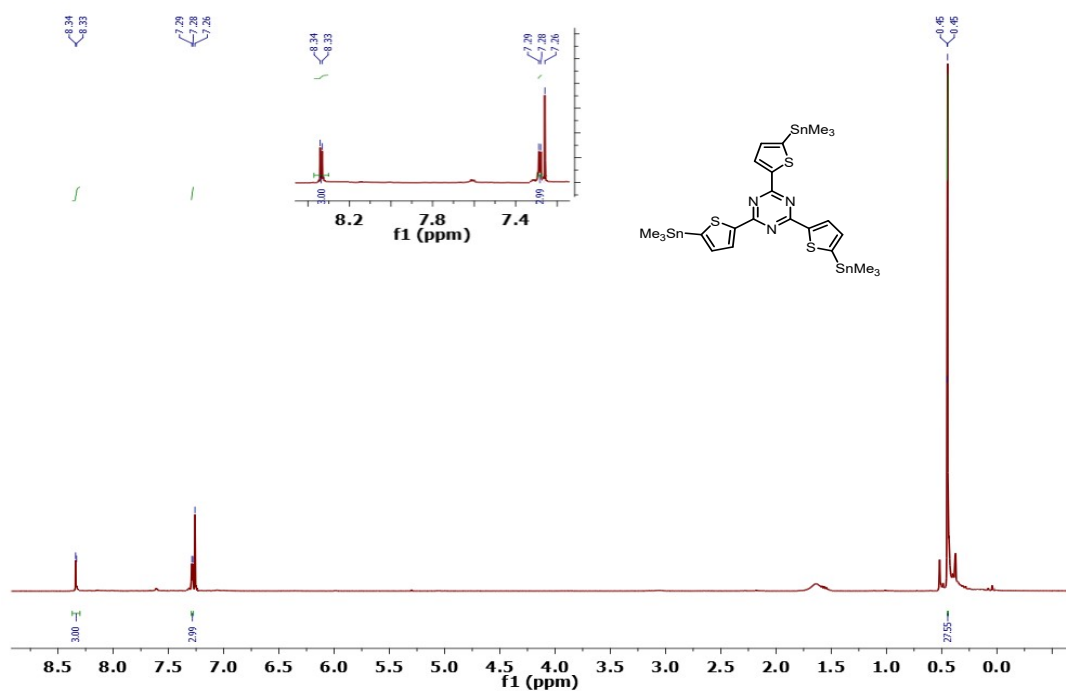


Fig. S14  $^1\text{H}$  NMR spectrum of 1 (400 MHz,  $\text{CDCl}_3$ ).



**Fig. S15**  $^1\text{H}$  NMR spectrum of **3** (400 MHz,  $\text{CDCl}_3$ ).

## References

- <sup>1</sup> S. Yeganegi, M. Gholami, V. Sokhanvaran, *Mol. Simulat.*, 2017, **43**, 260–266.
- <sup>2</sup> R. Maragani, R. Misra, *Tet. Lett.*, 2013, **54**, 5399-5402.
- <sup>3</sup> H. Muraoka, M. Mori, S. Ogawa, *Phosphorus Sulfur Silicon Relat. Elem.*, 2015, **190**, 1382-1391.